

Multivacancy effects in the x-ray spectra of CH_3Cl

R. C. C. Perera,* J. Barth,† R. E. LaVilla, R. D. Deslattes, and A. Henins
Quantum Metrology Group, National Bureau of Standards, Washington, D.C. 20234

(Received 29 April 1985)

A high-efficiency x-ray spectrometer has been constructed with use of a curved crystal and a position-sensitive detector mounted along a Rowland circle. Results obtained for the Cl K absorption and fluorescent $K\beta$ emission of molecular CH_3Cl show previously unobtainable details. The gas target is excited by primary radiation from a demountable conventional x-ray tube. The use of different anode materials and the insertion of filters between x-ray source and target allow some variation of the primary excitation energy. By monitoring emission spectra for different primary excitation energies, we are able to attribute the newly observed absorption features to multivacancy excitations. Such modulations in the suprathreshold absorption cross section would complicate the extraction of structural information in an extended x-ray-absorption fine-structure (EXAFS) analysis.

I. INTRODUCTION

X-ray-absorption and -emission spectra of molecules are useful for electronic-structure investigations since they are closely connected with the molecular orbitals, provided that observed spectra are understandable in terms of single-vacancy transitions. However, even for simple systems this requirement is not fulfilled. X-ray satellites resulting from multivacancy transitions are superposed on single-vacancy transitions yielding a complex emission spectra whose quantitative interpretation in terms of molecular-orbital single-electron transitions is elusive. Recently, a threshold study of the $K\beta$ emission of argon was devoted to investigate multivacancy effects for elemental argon.¹ The argon gas was excited by monochromatized synchrotron radiation which was sequentially tuned through single- and multiple-vacancy ionization thresholds of the Ar K edge, while at the same time recording the fluorescent Ar $K\beta$ spectrum. In this way it was not only possible to disentangle single- and multiple-vacancy emission contributions but also to establish a close relationship between $K\beta$ -emission satellites and the suprathreshold structure of the absorption spectrum. This permitted detailed assignments of many of the features in both absorption and emission spectra to specific excited states.

Taking the threshold study of Ar as the starting point, the present work is intended to serve two purposes. Firstly, a threshold study of a simple molecular system appeared to be a natural extension of the earlier work.¹ We chose to study Cl K spectra in CH_3Cl since, in an ionic bonding picture, the spectra should have some resemblance to the Ar spectra. The Cl $K\beta$ spectra of CH_3Cl excited considerably above threshold are well established and preliminary near-threshold studies have also been communicated.^{2,3} Secondly, the present work is partly a feasibility study since, in contrast to the work on Ar, a synchrotron-radiation source was not utilized. Progress in the design of high-efficiency secondary monochromators, which accompanied and finally permitted the experiment

on Ar, made it possible to use laboratory x-ray sources. The combination of different anode materials and filters provides a primary excitation spectrum where effective excess energy can be varied to a limited extent.

II. EXPERIMENT

The x-ray spectrometer, shown in Fig. 1, consists of a Johann bent-quartz ($10\bar{1}0$) crystal ($2d=4.916$ Å) and a linear position-sensitive gas proportional counter⁴ mounted on a Rowland circle. The dispersing crystal was bent to a radius of 55.9 cm. The instrument is operated in a helium environment at atmospheric pressure. The spectrometer design permits coordinated motion of the detector relative to the crystal along a (moving) Rowland circle.⁵ The detector was operated with a counter gas consisting of a mixture of Xe (90 vol %) and CH_4 (10 vol %) at a pressure of 35 kPa (350 Torr); its imaging charac-

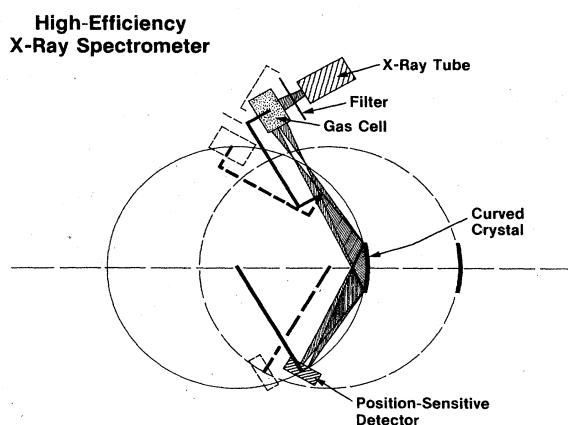


FIG. 1. Sketch of the high-efficiency x-ray spectrometer in fluorescence-emission mode. The shaded areas indicate focusing of x rays at two slightly different Bragg angles, measured simultaneously by the position-sensitive detector. The dashed lines refer to a situation where x rays at a grossly different Bragg angle are analyzed.

teristics were tested according to Ref. 4. The detector's position transfer function was found to be practically linear⁴ across the section used to record spectral data. The detector's spatial resolution of 100 μm was sufficient to adequately image the dispersed spectrum. A cell to contain the target gas and an x-ray tube were mechanically coupled to the x-ray spectrometer to provide an x-ray source outside the Rowland Circle. The demountable anode x-ray tube⁶ exciting the gas target operated typically at 15 kV and 200 mA for all fluorescent-emission spectra. To minimize the background due to generation of higher harmonic contributions, absorption spectra were taken with the high voltage of the tube limited to 5 kV. For the absorption measurements the x-ray tube was turned by 90° to point directly toward the analyzing quartz crystal with the 105-mm-long absorption-gas cell mounted in between. For both emission and absorption spectra, the target of flowing CH_3Cl gas was diluted with helium in the ratio of 1:10, at atmospheric pressure. This dilution ratio was empirically found to result in the maximum emission intensity with minimum distortion of the emission profile from self-absorption and to be thin enough that the "thickness effect"⁷ did not obscure the sharp features of the absorption spectrum. Commercially purchased gases were used without further purification.

An accurate calibration of the energy scale was conveniently obtained from the Pd $L\alpha_1$ emission line used in this experiment. The Pd $L\alpha_1$ -emission line⁸ at 2838 eV

was also used with the Cl $K\beta$ -emission spectrum² of CH_3Cl between 2810 and 2830 eV to establish the energy dispersion of the instrument. The resolution of the instrument in this region is 1.0 eV.

III. RESULTS

A typical example of the Cl $K\beta$ emission obtained in fluorescence and the Cl K -absorption spectra from CH_3Cl is shown in Fig. 2. The energies of the spectral components in Fig. 2 are listed in Table I. The Cl $K\beta$ -emission spectrum was excited by primary excitation from a Pd anode which was shown earlier to result in a minimum satellite contribution.^{2,3} Emission spectra with over 10^4 counts for the peak maximum are typically accumulated in less than 1 h. The ordinate of Cl K -absorption spectrum (Fig. 2) is μt obtained from measurements of I_0 and I of diluted CH_3Cl in the absorption cell. Typically the absorption measurements took 3–5 h to accumulate over 10^4 counts for each point in these two measurements. The absorption spectrum presented in Fig. 2 is a composite of two separate sets of measurements with a small change in Bragg angle to extend the absorption measurements to a higher-energy region.

We emphasize that the high efficiency of the curved crystal-position-sensitive detector spectrometer permits the observation of spectral features with excellent statisti-

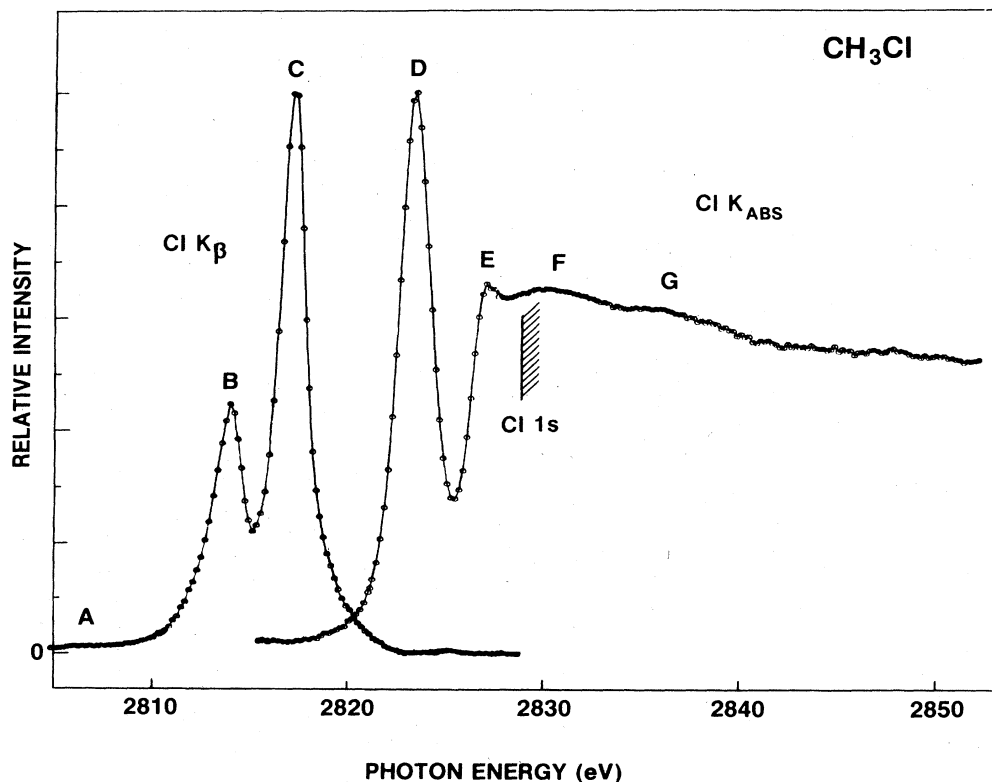


FIG. 2. The experimental chlorine $K\beta$ -emission and K -absorption spectra of CH_3Cl . The position of Cl $1s$ binding energy is indicated.

TABLE I. Major components in Cl $K\beta$ -emission and Cl K -absorption spectra of CH₃Cl molecule.

Peak	Energy (eV)
A	2806.4
B	2814.0
C	2817.2
D	2823.4
E	2827.4
F	2831
G	2836
Cl 1s	2828.5 ^a

^aReference 9.

cal quality accumulated in a reasonable amount of time. The procedure gives results that are substantially independent of drift in primary-source intensity. For comparison, Fig. 3 shows the Cl K -absorption and $K\beta$ -emission spectra obtained with a double-crystal spectrometer.⁹ The statistical scatter apparent from the data points above the ionization limit prevents any conclusion on weak suprathreshold structures in Fig. 3. Weak features such as the two broad maxima *F* and *G* are far more easily discernible in the spectrum of Fig. 2 than in the earlier measurements.^{9,10}

The Cl $K\beta$ -emission spectrum reveals new details but the principal features remains consistent with earlier measurements. In Fig. 4 we compare the Cl $K\beta$ spectrum excited with a Pd and a Sn anode; the emission spectra of Pd and Sn are dominated by their respective $L\alpha_1$ emission lines. The Pd $L\alpha$ has an energy⁸ of 2838 eV which is just above the Cl K threshold (2828.5 eV), while the

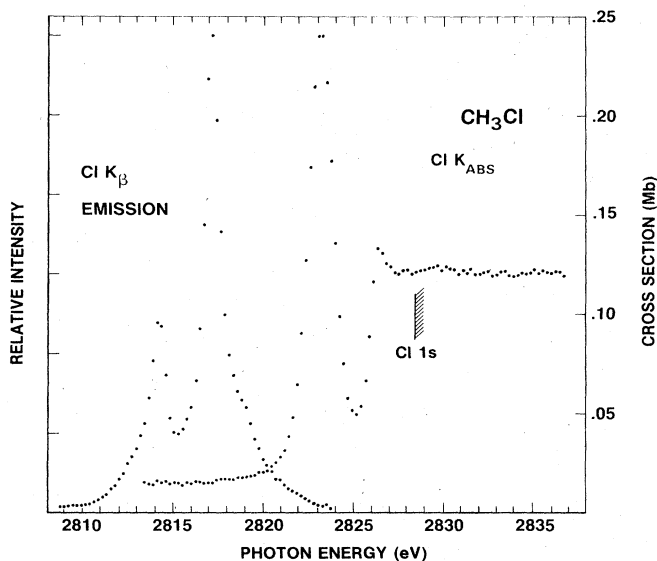


FIG. 3. Cl K -absorption (right) and Cl $K\beta$ -emission (left) spectra for CH₃Cl as obtained with a double-crystal monochromator (Ref. 9). The Cl 1s ionization threshold is also shown; the emission spectrum was excited by a Ag anode.

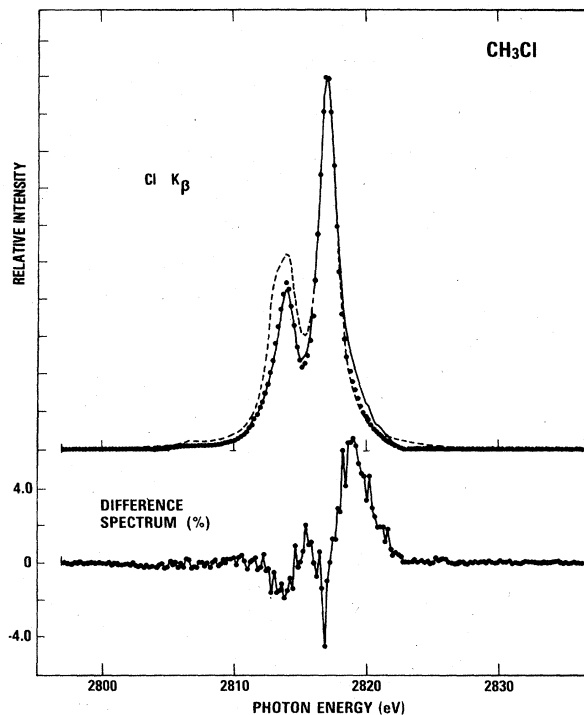


FIG. 4. Cl $K\beta$ emission of CH₃Cl excited by a Pd anode (dots) and a Sn anode (solid curve). Also shown is the result of a molecular-orbital calculation (dashed curve). All spectra are normalized to the peak intensity. The energetic width of the transitions is fitted to the experiment at the high-energy structure. In the lower panel the difference spectrum between the Sn-excited and Pd-excited Cl $K\beta$ spectra is displayed.

Sn $L\alpha$ -emission line at 3444 eV lies far above the Cl K threshold. Higher excess energy (over the Cl K ionization threshold) leads to a larger satellite contribution to the $K\beta$ -emission spectra due to the more probable excitation of multiple-vacancy states.² We obtain the spectral distribution of Cl $K\beta$ satellites as the difference between the normalized Pd excited and Sn excited Cl $K\beta$ -emission spectra (Fig. 4, lower part). The main satellite emission band thus obtained is located on the high-energy side of the single-vacancy spectrum; however, we also see some distortion of the single-vacancy spectrum itself due to the satellite emission. This could not be established previously, due to statistical scatter of the data points and irreproducibility of these spectra in earlier work.²

Also shown in Fig. 4 is a synthesized single-vacancy Cl $K\beta$ spectrum of CH₃Cl based on a molecular-orbital (MO) calculation. The semiempirical MINDO/3 method¹¹ (modified intermediate neglect of differential overlap) with complete geometry optimization constrained only to preserve the molecular point symmetry and a minimal valence basis set (without Cl 3d orbitals) was used in this calculation. The Cl $K\beta$ radiative yield values follow from the Cl 3p-orbital contributions to each molecular orbital as obtained directly¹² from the eigenvectors of the MINDO/3 MO calculation. The single-

vacancy¹³ Cl $K\beta$ spectrum is then synthesized from the calculated Cl $K\beta$ radiative yield values and experimental MO binding energies from ultraviolet-photoemission spectra,¹⁴ and broadened by a Lorentzian function having a 1.5 eV full width at half maximum¹² (FWHM). The same type of calculation was used successfully in analyzing the C K - and Cl $L_{2,3}$ -emission spectra¹⁵ of CCl_4 and CHCl_3 and found to be adequate at this level of analysis.

From the comparison of the experimental results for both small and large excess exciting-radiation energies, it is clear that the remaining discrepancies between calculation and experiment are significantly larger than the distortion of the experimental spectrum due to the satellite contribution. To obtain a better quantitative agreement a more sophisticated theory is needed, specifically one which goes beyond the present ground-state MO approximations.¹²

IV. DISCUSSION OF THE SUPRATHRESHOLD ABSORPTION SPECTRUM

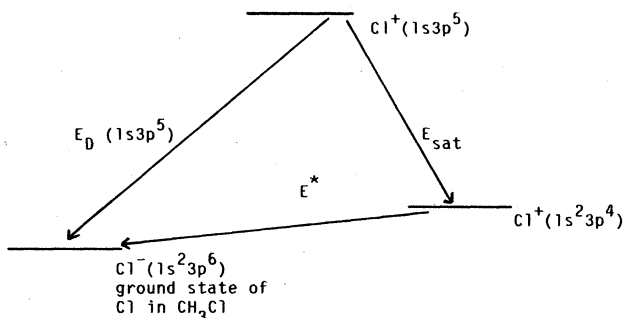
X-ray-absorption structure in the region about 40 eV above the core-ionization limit is usually attributed to transitions of single-core electrons to continuum states referred to as shape resonances,¹⁶ or to multivacancy transitions. Shape resonances are the precursor of the EXAFS (extended x-ray-absorption fine structure) features; however, the descriptions of shape resonances and EXAFS are not at present in the same language. A detailed calculation of the shape resonances for this molecule would be useful for comparison but is not available to our knowledge. Also, the limited range of the measured absorption spectrum does not permit a complete analysis in the EXAFS formalism.¹⁷ However, an estimate of the periodicity in the EXAFS structure can be obtained from the known interatomic distances of the molecular structure. The oscillatory part of the EXAFS is expressed¹⁷ as $\sin[2kr + \Psi(k)]$, where k is the wave vector of the photoelectron, r the distance of the neighboring atoms from the excited atom, and $\Psi(k)$ denotes a phase shift. Thus the periodicity in k space is given by $2k_p r = 2\pi$, or, energetically,

$$E_p = \frac{\pi^2 \hbar^2}{2mr^2}$$

In methyl chloride, the only important scattering center for photoelectrons from Cl ionization is the carbon atom, since the hydrogen atoms contain only small electronic charge. Thus, for CH_3Cl the expected EXAFS periodicity is 11.8 eV (Cl-C bond length¹⁸ is 1.78 Å), much larger than the observed 5-eV separation of the two maxima F and G , which is therefore not related to the EXAFS structure. This suggests that we should consider an interpretation of the suprathreshold feature based on multivacancy excitations. Unfortunately, no simple empirical rules can be applied to test the appropriateness of such an interpretation. While for free atoms the $Z + 1$ approximation works well to estimate thresholds for multivacancy excitations and even assign specific multiplets in suprathreshold absorption spectra,¹ the same approximation is not easily applicable to molecules. However, an estimate of the en-

ergy for the double-vacancy excitation can still be made.

If we associate the observed x-ray-emission satellite (Fig. 4) with the analogous transition for Cl^+ , namely $(1s3p^5) \rightarrow (1s^23p^4)$ (irrelevant electronic shells omitted), we can estimate the double-ionization threshold of $\text{Cl}^-(1s^23p^6) \rightarrow \text{Cl}^+(1s3p^5)$ using the first ionization potential of the molecule and the two-hole correlation energy of Cl. The calculation uses a closed cycle which can be represented by the following diagram:



where $E_D(1s3p^5)$ is the $1s3p$ double-ionization threshold, E_{sat} the x-ray transition energy of the $K\beta$ satellite, and E^* is the first double-ionization potential of Cl^- in CH_3Cl , which can be expressed as

$$E^* = 2E_I + U_{\text{corr},3p}$$

using the first ionization energy of a CH_3Cl molecule, E_I , and the two-hole correlation energy in the Cl $3p$ shell, $U_{\text{corr},3p}$. The first ionization potential of the molecule refers to the removal of an outermost electron from a $\text{Cl}^-(3p)$ -derived state.¹⁹ Therefore,

$$E_D(1s3p^5) = E_{\text{sat}} + (2E_I + U_{\text{corr},3p})$$

The correlation energy $U_{\text{corr},3p}$ can be inferred from atomic chlorine; its value equals the difference between the ionization energy of neutral Cl and twice the ionization energy of Cl^- . Using tabulated values^{20,21} for these ionization energies we find $U_{\text{corr},3p} = 5.4$ eV. Thus the estimated $1s3p$ double-ionization threshold is

$$\begin{aligned} E_D(1s3p^5) &= 2819 \text{ eV} + (2 \times 11.3 \text{ eV} + 5.4 \text{ eV}) \\ &= 2847 \text{ eV} \end{aligned}$$

which is 19 eV above the $1s$ single-vacancy ionization threshold. For Ar the corresponding double-ionization threshold is 31 eV above the single one, but the first two-hole bound state $\text{Ar}(1s3p^54s^2)$ lies only 15 eV above the $1s$ ionization limit.¹ Thus it appears possible that the broad absorption maximum about 8 eV above the Cl $1s$ threshold of CH_3Cl arises from a multivacancy complex.

Experimentally the relation between suprathreshold absorption structure and multivacancy excitation can be tested by scanning the energy of monochromatic primary radiation while at the same time recording fluorescence-emission spectra.¹ In the present experiment, a crude monochromatic analysis is permitted by the fortuitous location of the Ru L_3 edge^{8,22} in between the palladium

$L\alpha_1$ and $L\alpha_2$ characteristic emission lines.⁸ One has in this way the possibility to "tune" the excitation energy by selectively filtering out portions of the Pd $L\alpha$ radiation profile using Ru filters of different thicknesses.²³ The modified filtered primary radiation spectra are shown in the bottom part of Fig. 5. Observe that this radiation is located in the same energy region as the Cl K -absorption suprathreshold structure G of CH₃Cl (Fig. 5, middle panel; see also Fig. 2). For each primary excitation condition we recorded the Cl $K\beta$ -emission spectrum. The satellite emission intensity is obtained in the same way as previously described for Fig. 4, namely by subtraction of the normalized Cl $K\beta$ emission obtained with unfiltered Pd $L\alpha$ excitation. The shape of these difference spectra is similar to the one displayed in Fig. 4 for Pd and Sn primary excitation; however, the satellite intensity measured at 2819 eV and evaluated relative to the peak intensity of the Cl $K\beta$ emission varies significantly depending on the thickness of the Ru filter. By averaging over the energy distribution of the recorded primary excitation spectrum we associate a mean excitation energy with each primary excitation spectrum as shown by the vertical lines extending upward in the lower panel of Fig. 5. The upper right

panel of Fig. 5 gives the relative satellite intensities versus the mean primary excitation energy. For comparison we have included also the result with a Sn anode. The energy position of the Sn $L\alpha_1$ -emission line⁸ was taken as the mean primary excitation energy, which has an effective excess energy of 625 eV above the Cl $1s$ ionization threshold (Sn $L\alpha_1$: 3444 eV).

Before discussing the relative satellite-intensity variation with energy displayed in Fig. 5, we wish to make two further comments. Our measured satellite intensity is relative to the unfiltered Pd-excited Cl $K\beta$ spectrum. In the comparison between the Pd-excited Cl $K\beta$ spectrum and the MO calculation normalized to the main peak of the experimental spectrum shown in Fig. 4, the remaining relative satellite intensity is about 1% to 2%, compared to the maximum Cl $K\beta$ intensity. Secondly, our evaluation of the mean excitation energy completely neglects possible primary radiation from other Pd L -emission lines. While the $L\alpha$ emission is undoubtedly dominant, there is some contribution from these other Pd L primary x-ray lines,⁸ mainly from the $L\beta_1$ emission line ($3d \rightarrow 2p_{1/2}$; $E=2995$ eV). Higher-energy primary excitation radiation would result in an additional satellite intensity in our emission spectra. Of more serious consequence for our evaluation of relative satellite intensities, this higher-energy-produced satellite intensity will vary since the different filters used to modify the primary excitation do not attenuate Pd $L\alpha$ and higher-energy components equally. Therefore we checked the attenuation of the Pd $L\beta_1$ -emission line, which is the most prominent contaminating line radiation. The attenuation was found to be proportional to the $L\alpha_1$ attenuation for the Ru filters used in this experiment.

It thus appears that we have found a significant resonance for the excitation of the Cl $K\beta$ satellite at 2819 eV coincident with a weak, broad structure in the Cl K -absorption spectrum at around 2836 eV. This is the first clear identification of a suprathreshold feature in the x-ray absorption from a molecule with a multivacancy excitation complex of states linked to the emission satellite structure associated with its decay. Similar assignments¹ have been established for atomic argon where the absorption spectrum shows an array of relatively sharp features due to double-vacancy final states. For solid rare gases the double-vacancy excitations also exhibit structural features comparable to the gaseous argon absorption cross section,²⁴ and the Cl K multivacancy absorption structure of CH₃Cl therefore seems surprisingly weak and broad. Qualitatively we suggest that the breadth and absence of line structure are due to the Franck-Condon factors of the complex of excited states in the transitions. It is suggested that feature F in Fig. 2 is a shape resonance.

V. CONCLUSION

The present measurements show that the quality of x-ray-absorption and -emission spectra obtained with state of the art instrumentation, using conventional x-ray sources, is comparable to that obtained in synchrotron-radiation experiments. Certainly, the limited availability of intense line sources poses strong restrictions to systems which can be studied "at resonance." On the other hand,

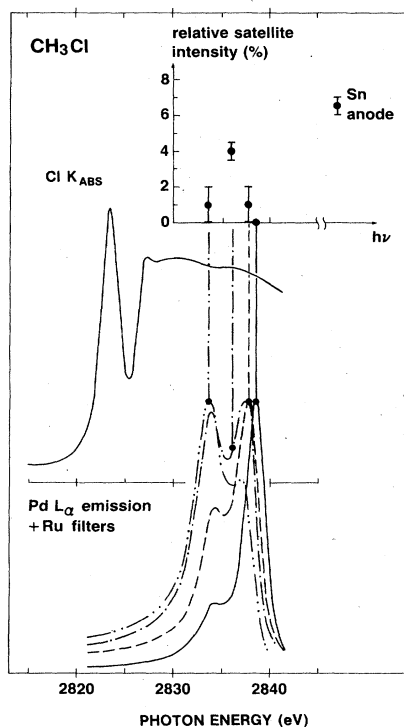


FIG. 5. Cl K absorption obtained at relatively high partial pressure of the sample gas to clearly expose the suprathreshold structure. In the lower part the primary radiation spectrum of the Pd $L\alpha$ emission is shown on the same energy scale modified by Ru filters: —, no filter; - - -, 1 μ m Ru; - · - · -, 2 μ m Ru; · · · · ·, 4 μ m Ru (Ref. 23). The inset in the upper part gives the relative intensity of the Cl $K\beta$ -emission satellite (for details see text), plotted versus a mean excitation energy obtained as a reasonable average of the primary radiation spectrum.

the lower cost of conventional laboratory equipment and easy access combine to give experimental setups such as the one described here—a residual importance even for x-ray-absorption and -emission measurements needing high statistical quality.

In summary, we have obtained the Cl $K\alpha$ -absorption and $K\beta$ -emission spectra of CH_3Cl with previously unobtainable details. We were able to identify a suprathreshold structure in the absorption spectrum as due to the excitation of multivacancy states whose decay in turn gives rise to satellites in the $K\beta$ -emission spectrum. It is hoped that the present results will stimulate molecular-orbital calculations of the excited final-hole states, not only to give a more satisfactory representation of the single-vacancy emission spectrum than the one presented here using a semiempirical calculation, but also to fully explore the dynamics of the photoexcitation process.

Finally, the result of the present investigation issues a clear warning with respect to interpretation of EXAFS

structures. The opening of multivacancy excitation channels above the single-vacancy absorption threshold may very well produce extra modulations of the suprathreshold absorption cross section which complicate the extraction of structural information in an EXAFS analysis. Recent evidence for such complications has also been presented for Ni-Zr alloys.²⁵ To fully disentangle the two contributions for the suprathreshold absorption structures in molecules and solids, in general, requires tunability available only with synchrotron-radiation sources.

ACKNOWLEDGMENTS

We would like to thank Professor Carl Nordling for stimulating discussions and comments on the manuscript, and one of the authors (R.C.C.P.) acknowledges the support by the U.S. Department of Energy (Contract No. DE-AC03-76SF00098) in preparation of this report.

*Present address: Center for X-ray Optics, Lawrence Berkeley Laboratory, University of California, Berkeley, CA 94720.

†Present address: BESSY Lentzealle 100, D-1000 Berlin 33, West Germany.

¹R. D. Deslattes, R. E. LaVilla, P. L. Cowan, and A. Henins, *Phys. Rev. A* **27**, 923 (1983).

²R. D. Deslattes and R. E. LaVilla, *Appl. Opt.* **6**, 39 (1967).

³R. E. LaVilla, *Advances in X-Ray Spectroscopy*, edited by C. Bonnelle and C. Mande (Pergamon, New York, 1982), p. 240.

⁴B. P. Duval, J. Barth, R. D. Deslattes, A. Henins, and G. G. Luther, *Nucl. Instrum. Methods* **222**, 274 (1984).

⁵R. D. Deslattes, R. E. LaVilla, and A. Henins, *Nucl. Instrum. Methods* **152**, 179 (1978).

⁶R. D. Deslattes and B. G. Simson, *Rev. Sci. Instrum.* **37**, 753 (1966).

⁷L. G. Parratt, C. F. Hempstead, and E. L. Jossem, *Phys. Rev.* **105**, 1228 (1957).

⁸J. A. Bearden, *Rev. Mod. Phys.* **39**, 78 (1967).

⁹The Cl $K\beta$ -absorption spectrum was obtained by step scanning with a double-crystal spectrometer [R. D. Deslattes, *Rev. Sci. Instrum.* **38**, 616 (1967)] equipped with calcite crystals. The sample gas CH_3Cl was contained in a 5.1-cm-long cell by 25- μm -thick beryllium windows at a pressure of 19 Torr. The continuum was provided by a gold-coated copper anode operating at 20 kV and 110 mA, and the radiation was detected with a flowing-gas proportional counter using P-10 counter gas (90 vol % argon, 10 vol % methane). The Cl $K\beta$ emission has been previously reported (see Ref. 2).

¹⁰M. J. Hanus and E. Gilberg, *J. Phys. B* **9**, 137 (1976).

¹¹R. C. Bingham, M. J. S. Dewar, and D. H. Lo, *J. Am. Chem. Soc.* **97**, 1285 (1975).

¹²R. C. C. Perera and R. E. LaVilla, *J. Chem. Phys.* **81**, 3375 (1984).

¹³R. Manne, *J. Chem. Phys.* **52**, 5733 (1970).

¹⁴A. W. Potts, H. J. Tempka, D. G. Street, and W. C. Price, *Philos. Trans. R. Soc. London, Ser. A* **268**, 59 (1970).

¹⁵R. C. C. Perera and B. L. Henke, *J. Chem. Phys.* **70**, 5398 (1979).

¹⁶J. L. Dehmer, *J. Chem. Phys.* **65**, 5327 (1976).

¹⁷*EXAFS Spectroscopy, Techniques and Applications*, edited by B. K. Teo and D. C. Joy (Plenum, New York, 1981).

¹⁸C. C. Costain, *J. Chem. Phys.* **29**, 864 (1958).

¹⁹G. Herzberg, *Electronic Spectra and Electronic Structure of Polyatomic Molecules* (Van Nostrand, Princeton, 1966).

²⁰C. E. Moore, *Atomic Energy Levels*, Natl. Bur. Stand. (U.S.) Circ. No. 467 (U.S. GPO, Washington, D.C., 1949).

²¹C. Weissmantel and C. Hamann, *Grundlagen der Festkörperphysik* (VEB deutscher Verlag der Wissenschaften, Berlin, 1979).

²²J. Barth, R. C. C. Perera, R. E. LaVilla, and C. Nordling (unpublished).

²³Effective thickness of the Ru filters were estimated by the attenuation of Cu $K\alpha$ radiation.

²⁴P. Rabe *et al.*, in a poster presentation at the International Conference on X-Ray and Atomic Inner-Shell Physics, University of Oregon, Eugene, Oregon, USA, August 23–27, 1982 (unpublished).

²⁵R. Frahm, R. Hansel, and P. Rabe, *J. Phys. F* **14**, 1029 (1984).